

# An Efficient Technique to Remove the Acid Gases from Natural Gas with Hollow Fiber Based Membrane-Assisted Gas Absorption Unit

Anton N. Petukhov<sup>1, 2\*</sup>, Artem A. Atlaskin<sup>1</sup>, Kirill A. Smorodin<sup>1, 2</sup>, Maria E. Atlaskina<sup>1, 2</sup>, Dmitriy M. Zarubin<sup>1, 2</sup>, Sergey S. Kryuchkov<sup>1</sup>, Anna N. Stepakova<sup>1</sup>, Andrey V. Vorotyntsev<sup>2</sup>, Olga V. Kazarina<sup>1, 2</sup>, Sergey S. Suvorov<sup>2</sup>, Ekaterina A. Stepanova<sup>2</sup>, Ilya V. Vorotyntsev<sup>1</sup>

<sup>1</sup>Mendeleev University of Chemical Technology of Russia, Miusskaya square, 9, Moscow, 125047 Russia

<sup>2</sup>Lobachevsky State University of Nizhny Novgorod, 23 Gagarin Avenue, Nizhny Novgorod, 603950, Russia

**Abstract.** This paper discusses the development and optimisation of the novel technique - membrane-assisted gas absorption (MAGA) and its application in the process of acid gases removal from natural gas, also known as natural gas sweetening process. Membrane-assisted gas absorption is a hybrid separation technique, which involves the selective absorption of acid gases with it further permeance through the membrane. It is pressure-drive heat-free method, which occurs continuously in a steady-state mode. The application of a new gas separation cell design, which is based on different hollow-fiber membranes (polysulfone gas separation and ultra-filtration) is discussed. That allows to decrease the ratio between the amount of absorbent and the area of the membrane in contact with it. The applied membranes and the cell itself were characterized with mass-spectra method to obtain mass transfer properties with respect to mixed gas. The absorbents were studied as well, and the absorption capacity and viscosity were obtained. Based on these experimental data the optimal membrane-absorbent system design was determined. Further, the separation efficiency of the membrane-assisted gas absorption technique was investigated on model (methane, carbon dioxide and xenon in the ratio of 94.5/5.35/0.15 vol.%) and quasi-real (methane, ethane, carbon dioxide, propane, nitrogen, butane, hydrogen sulfide and xenon in the ratio: 75.677/7.41/5.396/4.534/3.013/2.469/1.389/0.113 vol.%) gas mixtures. For both mixtures, the MAGA unit with 30 wt.% MDEA aqueous solution showed high gas separation efficiency. It is shown that the MAGA unit can remove up to 96% of sour gases from the mixture. At the same time, the hydrocarbon losses do not exceed 1%, even in the maximum productivity mode. It is also noted that the overall efficiency of the process can be improved by using specific absorbents with aqueous solutions of amino alcohols.

**Keywords:** gas separation; hollow fibers; membrane-assisted gas absorption; natural gas processing; sweetening;

## 1. Introduction

The development of civilisation is directly linked to the process of energy generation. In view of the increasingly severe environmental situation, technologies related to waste-free or low-waste methods of energy production play an important role (Liang et al., 2022; Ostergaard et al., 2020; Si et al., 2022; ZOU et al., 2021). Natural gas is one of the most environmentally friendly organic energy sources (Bello and Solarin, 2022; Litvinenko, 2020; Shirazi et al., 2022). Due to the fact that natural gas deposits, both due to geological and other factors (e.g. the biota that became the origin of the deposit) always contain acid gases (CO<sub>2</sub> and H<sub>2</sub>S), there is a necessity to separate acid gases from natural gas. Acid gases reduce the calorific value of fuel and create environmental and technological hazards (Khan et al., 2021; Rahmani et al., 2023; Tikadar et al., 2021a, 2021b).

Acid gases removal is an important step in the preparation of natural gas for transportation and processing (Darani et al., 2021; Liu et al., 2020). The most common today method of purification of natural gas from polluting components is amino-alcohol

chemisorption (Berchiche et al., 2023; Ellaf et al., 2023; Ibrahim et al., 2022). This method has been actively used and developed for several decades. However, despite this, it has some inherent disadvantages (Davarpanah et al., 2020; Godin et al., 2021; Struk et al., 2020). Among the main disadvantages are high capital and operating costs, problematic regeneration of sorbents, low reliability of apparatuses, relatively high complexity of operation and maintenance, large footprint, the necessity of preliminary deep purification of gas, and significant environmental damage from the process of operation (Ghasem, 2020; G. Liu et al., 2021; Rochelle, 2024). Additionally, it is also worth noting that amine purification plants are economically efficient only for very large production facilities.

Membrane gas separation offers an attractive alternative to amine treatment. The important disadvantages of amine scrubbing, which were pointed above, are not present (Lei et al., 2020; Y. Liu et al., 2021a, 2021b; Makertihartha et al., 2022; V. M. Vorotyntsev et al., 2006; Vorotyntsev et al., 2009; Yahaya et al., 2020). Thus, the membrane gas separation method is a reagent- and heat-free technology, where acid gas removal can be carried out at ambient temperature using relatively inexpensive polymeric materials (Hazarika and Ingole, 2024; Jana and Modi, 2024; Kryuchkov et al., 2024; Sidhikku Kandath Valappil et al., 2021). An important limiting factor in the development of the membrane method is the interdependence of selectivity and process performance. In other words, the more efficient the separation is - the lower the rate of this process (Robeson, 2008). Two main approaches to the improvement of membrane separation methods can be distinguished (Khan et al., 2024; I. V. Vorotyntsev et al., 2006). Firstly, new membrane materials can be sought (Bashir et al., 2024; Niu et al., 2024; Otvagina et al., 2019; Singh et al., 2024). However, this approach is still limited by the interdependence of performance and selectivity. Secondly, new engineering solutions can be sought (Karamah et al., 2021; Kartohardjono et al., 2023).

The group of authors proposed a new method, membrane assisted gas absorption (MAGA). MAGA is a pressure-controlled hybrid process. In its framework, the separation is continuous - gases are absorbed by a liquid absorbent spread over a membrane. After absorption by the liquid, the gases permeate through the membrane. The separation of gas mixtures takes place without phase transitions, in a single stage and without the need to maintain high temperatures. Compared to conventional membrane gas separation, the use of liquid absorbent allows to increase the selectivity of the system. An important and significant feature of the method is the self-regeneration of the absorbent, which occurs naturally in the process of gas sorption-desorption cycle and its penetration into the submembrane space. Taking into account the above mentioned, the most significant influence on the process is the choice of membrane and liquid absorbent materials. This imposes some limitations on the possibility of their selection - it is necessary to take into account the mass transfer rate. This is due to the fact that many polymeric materials, being able to effectively separate gas mixtures, cannot provide the required process rate.

The MAGA method was initially proposed by a group of authors for the removal of acid gases and for the ammonia recovery and purification, and the apparatus was based on planar-framed membrane modules (Atlaskin et al., 2021a; Kryuchkov et al., 2021; Petukhov et al., 2021). Then, various improvements of this method were proposed - the application of hollow fiber membranes to solve the same problem, as well as usage of ionic liquids as a sorbent in the system (Atlaskin et al., 2020a; Petukhov et al., 2022). The present study investigates the feasibility of applying the MAGA method to the separation of natural gas flow from sour gases. Modules based on hollow fibers made of PSF and PEI+PI are applied and investigated in this work.

The present work deals with comprehensive study of materials and process during the separation of natural gas using novel hybrid technique – membrane-assisted gas

absorption. During that complex investigation the combined system, which consists of absorbent, gas separation and ultra filtration membranes was proposed and characterized with respect to its mass transfer properties. Further, the proposed system was implemented during the separation process. It was found, that membrane-assisted gas absorption technique may be considered as an attractive alternative to conventional methods.

## 2. Materials and Methods

### 2.1. Materials

In correspondence to the aim of the present study - evaluation of the membrane-assisted gas absorption technique for natural gas processing, namely, removal of acid gas impurities, special gas mixtures in stainless steel cylinders were prepared. The first mixture, designed for the preliminary study, contains three components: methane, carbon dioxide and xenon in the ratio of 94.5/5.35/0.15 vol.% under the pressure of 4 MPa. The second mixture, identical in composition to natural gas, as it was mentioned in Patent (Smetannikov et.al., 2010) contains eight components: methane, ethane, carbon dioxide, propane, nitrogen, butane, hydrogen sulfide and xenon in the ratio: 75.677/7.41/5.396/4.534/3.013/2.469/1.389/0.113 vol.% under the same pressure value. The gas mixtures were prepared using pure gases: nitrogen ( $\geq 99.999$  vol.%), methane ( $\geq 99.99$  vol.%), xenon ( $\geq 99.999$  vol.%), ethane ( $\geq 99.94$  vol. %), propane ( $\geq 99.98$  vol.%), butane ( $\geq 99.97$  vol.%), carbon dioxide ( $\geq 99.99$  vol.%), hydrogen sulfide ( $\geq 99.5$  vol.%) supplied by «NII KM» Ltd, «Vössen M I Y» Ltd, «Firma Horst» Ltd (Moscow, Russia).

A 30 wt.% aqueous solution of amino alcohol - methyldiethanolamine (MDEA) was used as a liquid absorbent in the process of acid gas capture using a membrane-assisted gas absorption unit. Methyldiethanolamine was provided by «Oka-Sintez» Ltd (Dzerzhinsk, Russia). Deionized water obtained with Millipore Direct-Q3 was used to prepare the solutions. Reagents were used without additional purification. Solutions were prepared using standard gravimetric method on analytical balance SHIMADZU AUW-220D.

In this work, hollow fiber membranes of polysulfone (PSF) purchased from Hangzhou Kelin Aier Qiyuan Equipment Co., Ltd. (Hangzhou, China), polyetherimide/polyimide blend (PEI + PI) hollow fibers provided by the Institute of Macromolecular Chemistry CAS (Prague, Czech Republic) in cooperation with MemBrain s.r.o. company) were investigated. The studied membranes based on polysulfone and a polymer blend of polyetherimide (ULTEM 1000) and polyimide (Matrimid 5218) are hollow fibers with an anisotropic structure with an internal selective layer.

### 2.2. Methods

The schematic diagram of the experimental setup is shown in Fig. 1 and illustrates the membrane-assisted gas absorption unit, where the separation process is implemented in the counter-current flow mode. The schematic diagram of the separation cell, its detailed description, technical data, flat and 3D schemes and photos are given in Supplementary Materials (Fig. S1 – S2, Table S1). The source and product flows, which are feed and retentate, are controlled by mass flow controllers (Bronkhorst, El-Flow Prestige FG-201CV) and pressure transmitters (Wika, S-20). The constant pressure level in the cell and product line is maintained by a back pressure regulator (Bronkhorst, EL-Press P-702CM). The pressure on the permeate side is process controlled value, and is formed by the resistance in the fibers and the flow of permeate gas. In other words, the operator does not influence the pressure value manually. The outlets of the cell, which are permeate and retentate lines,

are connected to a four port two position switching valve (VICI, A4VL4MWE2) equipped with a high-speed switching accessory that allows 8 ms switch performance. It is used to alternately switch the analyte flows using a gas chromatography system. HSSA does not create pneumatic resistance in the line, which is typical for conventional valves, where the switching time exceeds 180 ms. The analyzed flow is fed into an analytical system represented by a Chromos GC-1000 gas chromatograph. There, the sample is separated in the chromatographic column under isothermal conditions and the signal change is recorded with a thermal conductivity detector. Detailed conditions for GC analysis are given in Table 1.

**Table 1** Process parameters for GC analysis

GC Component	Description
Detector	TCD-1, 3V, 170°C TCD-2, 3V, 170°C
Analytical Column	Hayesep R 3m×2mm, SS316 stainless steel (SS316), 80/100 mesh Hayesep Q 3m×2mm, SS316 stainless steel (SS316), 80/100 mesh 40°C (5.8 min) heat 25°C/min (0.8 min); 60°C (3.6 min) heat 25°C/min (0.8 min); 80°C (2.5 min) heat 35°C/min (1.57 min); 135°C (9.9 min); 200°C
Sampling loop	1 cm <sup>3</sup> , 145°C
Carrier gas	He 99.995 vol.%, 20 cm <sup>3</sup> min <sup>-1</sup>

The experiment entails introducing the gas system into the inlet port of the experimental unit via a Drastar pressure regulator to uphold a desired pressure level prior to the mass flow controller, which guarantees an accurate gas flow rate of the separated gas mix. The feed stream enters the MAGA unit, where impurities of acid gases are captured by a combined membrane-absorption system, and transferred to the permeate side. Next, the separated components are captured with carrier gas fed through a pressure regulator and mass flow controller and exits the unit for further analysis. The same process is performed for the retentate, which is depleted of permeated components. The back pressure regulator mounted on the retentate line provides a consistent pressure level throughout the length of the line from its feed to the regulator, ensuring a uniform pressure ratio across the combined system. The permeate and retentate streams are sequentially analyzed via a gas chromatograph to assess the progression of achieving a steady state and the efficiency of the separation process. The experimental conditions are given in Table 2.

**Table 2** Experimental conditions over the membrane-assisted gas absorption process

Parameter	Value
Feed stream pressure	0.4 MPa
Permeate pressure	0.104 – 0.105 MPa
Feed flow rate	100 – 150 cm <sup>3</sup> min <sup>-1</sup>
Temperature	25°C
Stage-cut	0.05 – 0.065

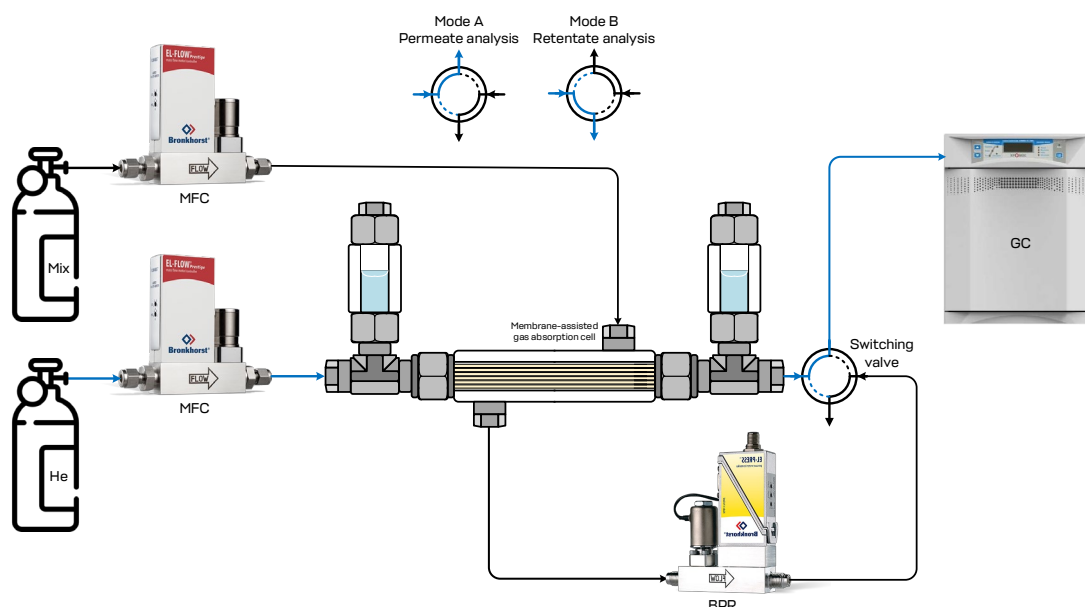


**Figure 1** The principal scheme of the experimental setup for the evaluation of separation process using MAGA technique

### 2.3. Determination of gas transport characteristics of the membrane

One of the main objectives of this study is to determine a suitable membrane considering its mass transfer properties (permeance, selectivity) and stability in the presence of plasticizing components such as carbon dioxide and hydrogen sulfide. The key requirement for the membrane is high permeance, as the high selectivity is provided by the liquid absorbent.

This study considers a new membrane-assisted gas absorption unit based on hollow fibers. Unfortunately, there is no production of hollow PVTMS (Atlaskin et al., 2021b, 2020b) fibers in the world, so it is very important to find a membrane with characteristics close to those specified. In addition, to date, there are very few studies containing data on the permeance of such membranes to the gases, which are considered as components of studied mixture, especially for hollow fibers. In this regard and in order to accurately determine a suitable membrane, an experimental study of the gas transport properties of asymmetric hollow fiber gas separation membranes made of polysulfone provided by Airrane Co., Ltd and polyethylenimine with polyimide was carried out.

The study of membrane materials was carried out on an experimental setup coupled with a residual gas analyzer Pfeiffer QMG 250. The general scheme of the unit is presented in Figure 2. The setup is equipped with three mass flow controllers (Bronkhorst FG-201CV) for supplying pure gases. These controllers can be used either individually or in gas mixing mode. The gas mixture, in turn, is obtained by real-time dynamic flow mixing. Two more controllers (Bronkhorst F201CV and Bronkhorst F201CM) are used to supply helium and argon to the experimental setup (in the case when the permeance of these gases is not the object of research). Helium is used to purge the gas distribution system of the setup between tests. Argon is used as an internal standard in the mass spectrometer. A two-position, four-port valve is used to connect the module's feed side to the mixing chamber or helium inlet line. The retentate line of the module is connected to back pressure regulator (Bronkhorst P702CM) to maintain a constant target pressure value. The permeate side of the module is connected to a pumping station consisting of a diaphragm and turbomolecular vacuum pump (Pfeiffer Hi-Cube ECO 300). The vacuum level on the

permeate side is measured with a pressure transmitter (Pfeiffer MPT200). A solenoid-operated diaphragm valve installed between the cell and the vacuum station (Pfeiffer DVC 025 PX) is used to shut down the vacuum equipment in case of pressure surges resulting from damage to the membrane samples. The vacuum system is then connected to the mass spectrometer chamber (Pfeiffer PrismaPro QMG 250 M2), where the vacuum is provided by a second pumping station (Pfeiffer Hi-Cube 80 Eco) and its vacuum level is determined by a second pressure transmitter of the same model.

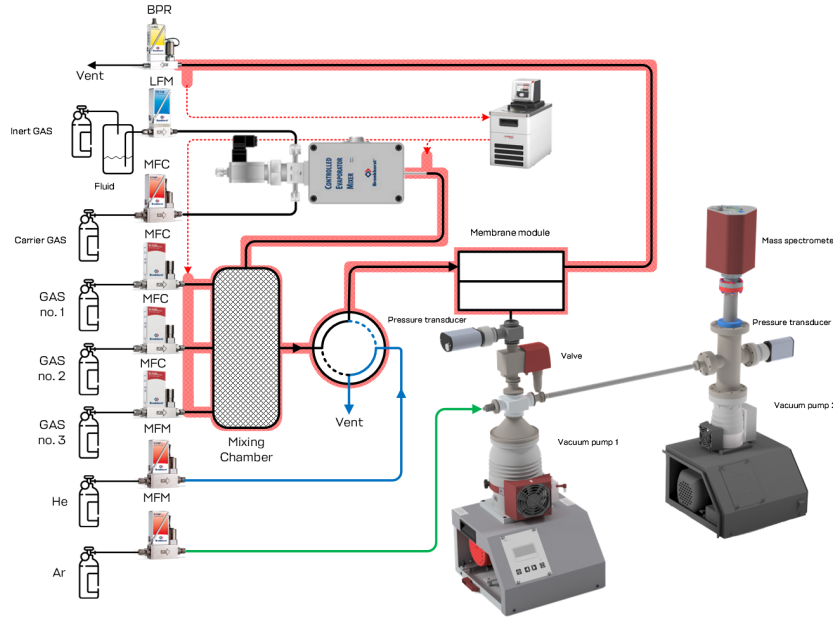


**Figure 2** Schematic diagram of mass spectrometer coupled experimental unit for membrane mass transfer properties study

Before each experiment, the test cell is purged with helium (at a volume flow rate of 50 - 150 cm<sup>3</sup> min<sup>-1</sup>). The mixing chamber is filled with individual gas or multiple gases (total volume flow rate - up to 750 cm<sup>3</sup> min<sup>-1</sup>). Argon is also supplied to the vacuum side of the gas distribution system (volume flow rate 4 cm<sup>3</sup> min<sup>-1</sup>), unless an argon permeance study is required. Helium purging is necessary to remove air or gases remaining in the system after previous experiments. The removal process is monitored by a mass spectrometer that records the spectrum in real time with a 1 ms update delay. At the end of the purge procedure, the two-position valve is switched to the position where the mixing chamber is connected to the feed side of the cell. The switching time of the valve is 8 ms. The gas pressure in the cell's feed side and the gas volume flow rates are monitored using the FlowPlot software, the pressure in the permeate side and in the mass spectrometer chamber are monitored using the PV TurboViewer software, and the mass spectra are monitored using the PV MassSpec software. Thus, all experimental data are collected to determine the gas transport characteristics of the membrane.

Permeance  $Q$  (cm<sup>3</sup> cm<sup>-2</sup> s<sup>-1</sup> cmHg<sup>-1</sup>) is calculated by the formula (see equation 1):

$$Q = \frac{J_i}{\Delta p_A} \quad (1)$$

where  $J_i$  is the volumetric flow rate of component  $i$  in the permeate, cm<sup>3</sup> s<sup>-1</sup>;  $\Delta p$  is a difference in partial gas pressures across the membrane, cmHg; and  $A$  is the membrane area, cm<sup>2</sup>.

Selectivity is calculated by the formula (see equation 2):

$$\alpha = Q_A/Q_B \quad (2)$$

where  $Q_A$  and  $Q_B$  are the values of permeance of gases  $A$  and  $B$ ,  $\text{cm}^3 \text{ cm}^{-2} \text{ s}^{-1} \text{ cmHg}^{-1}$ . The software of the mass spectrometer allows transformation of the signal of each component into the value of its partial pressure. Thus, the permeate volumetric flow rate may be estimated by the formula (see equation 3):

$$\frac{J_i}{J_{Ar}} = \frac{p_i}{p_{Ar}} \quad (3)$$

where  $J_{Ar}$  is the volumetric flow rate of argon,  $\text{cm}^3 \text{ min}^{-1}$ ;  $p_i$  is the partial pressure of component  $i$  in the permeate,  $\text{cmHg}$ ; and  $p_{Ar}$  is the partial pressure of argon in the permeate,  $\text{cmHg}$ . The error does not exceed  $\pm 2.2\%$  of the measured value.

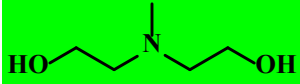
After the permeation tests were performed for hollow fibers, the membrane-assisted gas absorption cell was studied. The mass transfer properties of the cell were determined according to the technique described above. As the permeate side of the cell is flow-through volume, the helium sweep inlet was stubbed in order to perform vacuum mode measurements.

### 3. Results and Discussion

#### 3.1. Preliminary tests of absorbent solution

In this work, aqueous solutions of methyldiethanolamine were investigated as an absorbent. A special feature of MDEA is that it can be partially regenerated in an instant. As a result, removal of large amounts of acid gases can be achieved with a small amount of heat for regeneration (desorption temperature 373 K) (Jamal et al., 2006). Since MDEA is a tertiary amine, it has a lower affinity for  $\text{H}_2\text{S}$  and  $\text{CO}_2$  than DEA. MDEA has several distinct advantages over primary and secondary amines. In addition, MDEA is characterized by higher resistance to decomposition. The slowness of the reaction leading to the formation of bicarbonate is the main reason why tertiary amines can be considered as selective for the removal of  $\text{H}_2\text{S}$ , in cases where complete removal of  $\text{CO}_2$  is not required. The chemical properties of MDEA are presented in Table 3.

**Table 3** Chemical properties of MDEA

Amines	CAS number	Chemical structure	MW(g/mol)
N-methyldiethanolamine (MDEA)	105-59-9		119.16

The mechanism of acid gas sorption by amino alcohols is illustrated by the reaction of primary amines with  $\text{CO}_2$  and  $\text{H}_2\text{S}$  (formulas 1-5).



With primary and secondary amines, the dominant general reaction (equation 1) quickly leads to the formation of a stable carbamate, which is slowly hydrolyzed to



bicarbonate. The other general reactions leading to the formation of bicarbonate (equation 2) and carbonate (equation 3) are slow because they must go through the hydration of CO<sub>2</sub>.

Unlike primary and secondary amines, the nitrogen in tertiary amines does not have free hydrogen for the rapid formation of carbamate according to the general equation (1). As a consequence, CO<sub>2</sub> removal by tertiary amines can only occur via the slow pathway to bicarbonate according to equation (2) and carbonate according to equation (3). The slowness of the reaction leading to bicarbonate formation is the main reason why tertiary amines can be considered selective for H<sub>2</sub>S removal when complete CO<sub>2</sub> removal is not required. However, at high partial pressures, the solubility of CO<sub>2</sub> in tertiary amines is much higher than in primary and secondary amines.

As a part of the complex study, the preliminary tests of absorbent systems were performed. In order to choose the most suitable absorbent the wide range of MDEA concentration in aqueous solution were considered and compared with literature data. The comparison was performed to verify the applied experimental technique and evaluate absorbent properties in conditions, which are close to the conditions of the separation process. In correspondence with that aim, the MDEA mass fraction was changed from 10 to 40 wt.% with a step of 10 wt.%, meanwhile the literature data is given for the 0 – 60 wt.%.

The appliance of MDEA is justified by a number of factors. MDEA also practically does not cause corrosion, is characterized by low saturated vapor pressure, has a low specific heat capacity and heat of reaction with H<sub>2</sub>S and CO<sub>2</sub>. As a result of using an aqueous solution of MDEA, with an amino alcohol mass content of 30%, in 1987 it was possible to reduce the carbon dioxide content in commercial gas to 1–1.4% as a result of processing the natural gas at the Orenburg and Karachaganak oil and gas condensate fields (OGCF) (Nasteka, 1996).

Moreover, based on the data available in the literature, it is evident, that 30% aqueous solutions of MDEA offers the highest absorption capacity among others alkanolamines, such as monoethanolamine (MEA) and triethanolamine (TEA). Table 4 contains values of 30% aqueous solutions of MEA, TEA and MDEA absorption capacity with respect to carbon dioxide.

**Table 4** Absorption capacity of various alkanolamines toward to carbon dioxide.

Alkanolamine	Absorption capacity		P, kPa	Reference
	$mol_{CO_2} \cdot mol_{amine}^{-1}$	$mol_{CO_2} \cdot kg_{abs}^{-1}$		
MEA	0.59	2.90	100	(Hadri et al., 2015a; Yamada et al., 2012)
	0.60-0.62	2.95-3.05	100	(Dawodu and Meisen, 1994; Jou et al., 1995; Mahi et al., 2019)
MDEA	0.68	1.71	100	(Fu et al., 2016a; Hadri et al., 2015a)
TEA	0.38	0.76	100	(Rayer et al., 2012)

The viscosity measurements were carried out on an Anton Paar MCR702e rheometer equipped with a PR170/Ti/XL measuring cell, a C-ETD 200/XL/PR temperature sensor and a PA-23S pressure sensor. Solutions of MDEA with mass concentration of 10 – 40 wt.% were prepared. Measurements were performed at a pressure of 100 and 400 kPa for neat and acid gases rich absorbents, respectively. The PR170/Ti/XL is measuring cell made of



titanium and allows to perform measurements at elevated pressure values. In that case, the viscosity measurement of loaded MDEA aqueous solutions were performed in the environment of eight component gas mixture.

Moreover, the present study deals with the evaluation of MDEA aqueous solutions CO<sub>2</sub> absorption capacity with different MDEA mass concentration (similar to described above). The absorption capacity of solutions was calculated based on the raw data obtained from gravimetric technique. The weight gain was measured using analytical balance (VIBRA AF-225DRCE) (Accuracy:  $1 \cdot 10^{-4}/1 \cdot 10^{-5}$  g). Aqueous solutions were loaded into a thin-wall stainless steel cuvette with connectors for gas inlet and outlet. The outlet tube is connected with back pressure regulator (Bronkhorst P702CM) which maintains the constant pressure during the experiment. After the weight of the sample stops to change, the solubility limit is reached, and the total weight gain is the absorption capacity of the sample. The cell was placed in a thermostat and maintained at a constant temperature of 298.15 K. The experiment was carried out at atmospheric pressure ( $\sim 100$  kPa) and at elevated pressure of 400 kPa. The obtained results at atmospheric pressure were compared to literature data, and then, after the technique was verified, the absorption capacity at 400 kPa was investigated. The experimental scheme for absorption capacity measurements is given in Figure 3.

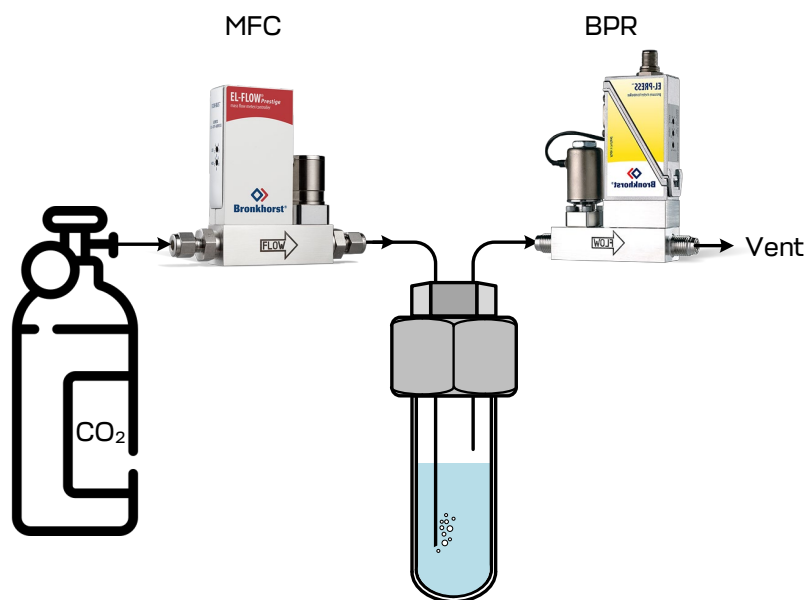


**Figure 3** The principal scheme of the experimental setup for absorption capacity measurements.

The results of preliminary study of absorbents are shown in Figure 4 (a, b), where the viscosity ( $\eta$ ) and absorption capacity ( $n_{CO_2} \cdot m_{abs}^{-1}$ ) plotted against MDEA mass fraction in aqueous solutions.

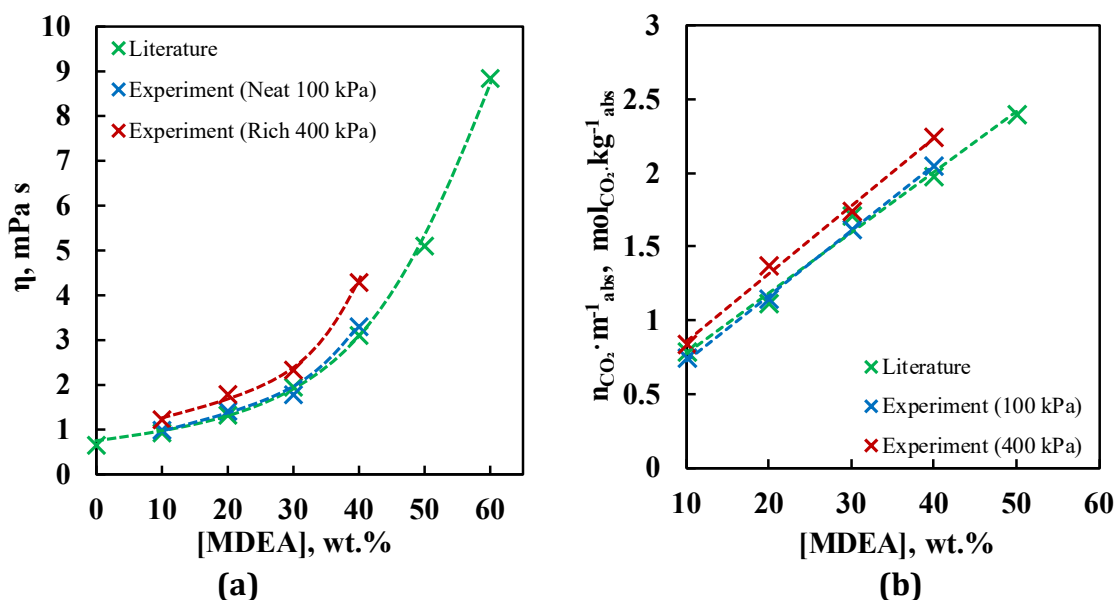


**Figure 4** The viscosity (a) and absorption capacity (b) of MDEA aqueous solutions with different MDEA mass fraction. Green crosses are literature data (Fu et al., 2016b; Hadri et al., 2015b); blue crosses are experimental data obtained in present study as a verification of techniques; red crosses are experimental data for loaded MDEA aqueous solutions under elevated pressure (left) and data obtained at elevated pressure during CO<sub>2</sub> absorption (right).

As is seen from the curves, given in Figure 4 (a), the experimentally obtained viscosity values of MDEA aqueous solutions under 100 kPa are close to data given in literature (Fu et al., 2016b; Hadri et al., 2015b). Thus, the deviation is no more than 9 % is observed, and, basing on these results it may be concluded, that applied technique provides correct measurements. Further, the measuring cell was fed with eight component mixture under the pressure of 400 kPa and was kept during 72 hours, to be sure, that the solution limit is reached. After that, the viscosity measurement was performed. It is seen, that the viscosity of rich MDEA aqueous solutions is higher, than the values obtained for neat samples in the whole observed range of solution composition. Thus, for 10 wt.% MDEA content it is 1.23, for 20 wt.% - 1.79, for 30 wt.% - 2.33 and for 40 wt.% it is 4.29 mPa s. According to the viscosity dependence on MDEA content, it is of interest to apply solution from linear region of viscosity gain – 10 – 30 wt.%. Increasing the MDEA content from 10 – 20 wt.% provides the increase in the viscosity value of 45.9 %, further increase of MDEA content to 30 wt.% accompanied with viscosity gain up to 84 %.

Thus, the higher viscosity of CO<sub>2</sub> loaded solutions is observed due to the increase in intermolecular forces between aqueous amine molecules, CO<sub>2</sub>, and reaction products.

The Figure 4 (b) illustrates the influence of MDEA content on the absorption capacity of different MDEA aqueous solutions. As is seen from the graphs, all considered cases are linear. There are three curves in the Figure: literature data; experimental data, obtained at the same conditions; experimental data obtained at the elevated pressure of 400 kPa. The experimentally found absorption capacity values at 100 kPa are in well agreement with literature data. And it allows to conclude, that the applied technique is appropriate and provides correct data. Further, the same tests were performed at the 400 kPa pressure of pure CO<sub>2</sub>. It was found, that the absorption capacity dependence is linear too and overcome the values obtained at 100 kPa. The absorption capacity gain was up to 23.4 % in comparison with literature data and values obtained at 100 kPa of CO<sub>2</sub>. Taking into account linear growth of the MDEA aqueous solutions CO<sub>2</sub> absorption capacity observed for all

considered compositions, the criteria of suitability is viscosity value, as it influences the mass transfer characteristics, namely the diffusion component.

According to the Stokes-Einstein-Sutherland equation, it is possible to evaluate the diffusion coefficients of gas into the liquid absorbent system:

$$D = \frac{k_B T}{6\pi\eta r^2} \quad (4)$$

where  $D$  is diffusivity coefficient of gas A in liquid B,  $\text{cm}^2 \text{s}^{-1}$ ;  $k_B$  – Boltzmann constant;  $T$  – temperature, K;  $\eta$  – dynamic viscosity, mPa s;  $r$  – particle radius, m. The Stokes-Einstein-Sutherland relation was used to calculate diffusion coefficients. For technological calculations, a factor of  $4\pi$  rather than  $6\pi$  is often used. It is important to point out that the values predicted by this equation are only estimates.

The results of the diffusion coefficients estimation are given in Figure 5. As is seen, the maximum values of  $\text{CO}_2$ ,  $\text{H}_2\text{S}$  and  $\text{CH}_4$  diffusion coefficients are observed at 10 wt.% MDEA content. Increasing MDEA concentration to 30 wt.% the diffusion coefficients decrease almost twice (1.9 times) in comparison with 10 wt.% MDEA aqueous solution, meanwhile at 40 wt.% MDEA content, the diffusion coefficients are 3.5 times lower. Wherein, the absorption capacity of 30 wt.% MDEA content, the absorption capacity is 2.1 times higher, then 10 wt.% MDEA aqueous solution. Increasing the MDEA content up to 40 wt.%, the absorption capacity increases 2.7 times. Taking into account the complex of obtained results, it may be concluded, that the optimal absorbing solution composition is 30 wt.% MDEA aqueous solution.

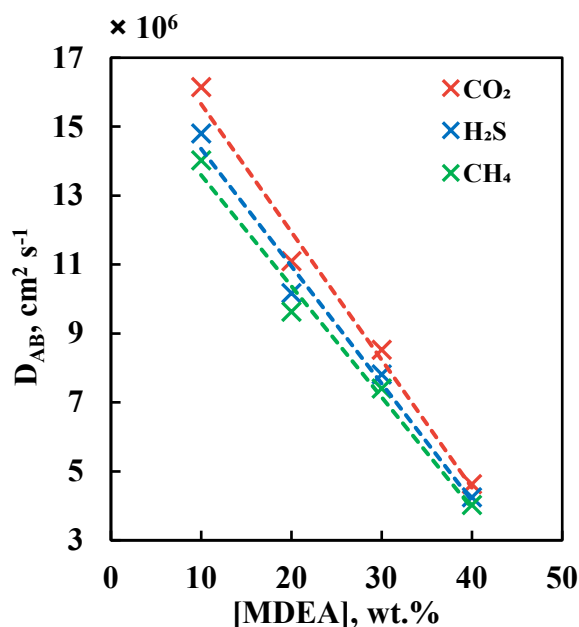


**Figure 5** The ideal gas diffusion coefficient in MDEA aqueous solution in dependence of MDEA content for  $\text{CO}_2$  loaded absorbent

### 3.2. Determination of permeance

According to the results of the study for hollow fiber membranes PSF and PEI + PI the permeance values for a number of gases included in the considered gas mixtures were determined and the results are shown in Tables S2 – S5 in supplementary materials. It was determined that the polysulfone hollow fiber has higher permeance values for all the considered gases. Thus, for the polysulfone membrane, the permeance decreases in the series  $\text{CO}_2 > \text{H}_2\text{S} > \text{C}_4\text{H}_{10} > \text{CH}_4 > \text{C}_2\text{H}_6 > \text{N}_2 > \text{C}_3\text{H}_8 > \text{Xe}$  and are 322.1, 244.3, 37.2, 30, 22.9,

22.3, 16.9 and 11.2 GPU, respectively. At the same time, the PEI+PI membrane permeance values decrease in the series  $\text{CO}_2 > \text{H}_2\text{S} > \text{CH}_4 > \text{C}_2\text{H}_6 = \text{C}_3\text{H}_8 = \text{C}_4\text{H}_{10} > \text{N}_2 > \text{Xe}$  and are 30.7, 13.6, 2.8, 2, 2, 2, 1.6 and 0.9 GPU, respectively. Thus, the permeance values of the PEI+PI membrane are lower than those of the PSF membrane by more than 90.5 %. At the same time, both membranes demonstrate comparable selectivity values.

Studying the gas transport characteristics of the components of the gas mixture, it was found that the permeance values of the PEI+PI membrane for all of the considered components practically do not change. For the PSF membrane a sharp increase in values is observed, which is most likely caused by plasticization of the membrane under the influence of carbon dioxide and hydrogen sulfide. At the same time, there is a significant decrease in selectivity of the membrane for all considered gas pairs. However, such values are retained during long-term operation of the membrane. Since the membrane permeance is the key characteristic determining the possibility of its application in the membrane-assisted gas absorption technique, polysulfone fibers are the most preferable option out of the considered ones.

Further, the mass transfer properties of overall membrane-assisted gas absorption cell were studied. The assembled cell was connected to the permeance experimental setup coupled with a residual gas analyzer. The connection was performed in accordance with scheme given in Fig. 1 with the exception of helium sweep inlet. It was stubbed and the permeate outlet was connected to vacuum line of permeance test setup.

The test was performed using the same eight-component gas mixture, and the results are given in Table 5. The permeance of the membrane-assisted gas absorption system dramatically decreases for all components of the mixture. It became almost impermeable for nitrogen, xenon and  $\text{C}_1 - \text{C}_4$  hydrocarbons, meanwhile the carbon dioxide and hydrogen sulfide pass the system. The system permeance with regard to  $\text{CO}_2$  and  $\text{H}_2\text{S}$  is 6.2 and 4.2 GPU, respectively. As a consequence, the selectivity of the combined system ( $\alpha(\text{CO}_2/x)$  and  $\alpha(\text{H}_2\text{S}/x)$ ) is much higher than PSF and PEI+PI membranes. For example, the  $\text{CO}_2/\text{CH}_4$  and  $\text{H}_2\text{S}/\text{CH}_4$  selectivity is 206.67 and 140.00 respectively. These results are explained by the presence of a layer of liquid absorbent, which interact prepensely only with acid components –  $\text{H}_2\text{S}$  and  $\text{CO}_2$ , meanwhile  $\text{N}_2$  and  $\text{C}_1 - \text{C}_4$  does absorbs in this MDEA aqueous solution. As is known, Xe has modest solubility in water, but, supposably in the presence of carbon dioxide (5.396 mol.%) and hydrogen sulfide (1.389 mol.%) provides the competitive sorption and xenon is very slightly absorbed by MDEA aqueous solution.

**Table 5** Mass transfer properties of the membrane-assisted gas absorption cell based on the PSF hollow fibers.

Q, GPU <sup>a</sup>							
N <sub>2</sub>	CH <sub>4</sub>	Xe	C <sub>2</sub> H <sub>6</sub>	C <sub>3</sub> H <sub>8</sub>	C <sub>4</sub> H <sub>10</sub>	CO <sub>2</sub>	H <sub>2</sub> S
0.02	0.03	-	0.02	0.02	0.02	6.2	4.2
α (CO <sub>2</sub> /x)							
CH <sub>4</sub>	C <sub>2</sub> H <sub>6</sub>	C <sub>3</sub> H <sub>8</sub>	C <sub>4</sub> H <sub>10</sub>	N <sub>2</sub>	H <sub>2</sub> S		
206.67	310.00	310.00	310.00	310.00	1.48		
α (H <sub>2</sub> S/x)							
CH <sub>4</sub>	C <sub>2</sub> H <sub>6</sub>	C <sub>3</sub> H <sub>8</sub>	C <sub>4</sub> H <sub>10</sub>	N <sub>2</sub>	CO <sub>2</sub>		
140.00	210.00	210.00	210.00	210.00	0.68		

@ pressure drop 400 kPa, 25 °C.

<sup>a</sup>1 GPU =  $1 \times 10^{-6} \text{ cm}^3 \text{ cm}^{-2} \text{ s}^{-1} \text{ cm Hg}^{-1}$

**Table 6** Mass transfer properties of the membrane-assisted gas absorption cell in a comparison with supported ionic liquid membranes.

System	Q, GPU	$\alpha$
--------	--------	----------

	CH <sub>4</sub>	N <sub>2</sub>	CO <sub>2</sub>	H <sub>2</sub> S	CO <sub>2</sub> /CH <sub>4</sub>	CO <sub>2</sub> /N <sub>2</sub>	H <sub>2</sub> S/CH <sub>4</sub>	H <sub>2</sub> S/N <sub>2</sub>
Present study*	0.03	0.02	6.2	4.2	206.67	310.00	210.00	210.00
Nanoporous aluminum with [BMIM][Ac]**			54			5.4		
Porous aluminum oxide + phenolic resin with [EMIM][BF <sub>4</sub> ]**			0.182			40		
Graphene oxide with [BMIM][BF <sub>4</sub> ]**			68.5		234	382		
Polyimide P-84 with [APTMS][Ac]**			23		41			
$\gamma$ -alumina and [EMIM][FAP]**			208		3			

\* - @ pressure drop 400 kPa, 25 °C.

\*\* - literature data (Friess et al., 2021)

As a result of mass transfer characteristics comparison between combined membrane-assisted gas absorption system and supported ionic liquids membranes (Table 6), as another class of barrier with liquid layer, it is evident that the system under study is characterized by moderate permeability values. Thus, the CO<sub>2</sub> permeability of the system under consideration is 6.2 GPU, which is higher than the value obtained for porous aluminum oxide with phenolic resin and [EMIM][BF<sub>4</sub>] (0.182 GPU), but lower than the same value for other SILMs. At the same time, the system under study achieves the highest selectivity for CO<sub>2</sub>/N<sub>2</sub> and CO<sub>2</sub>/CH<sub>4</sub> pairs. Comparison for H<sub>2</sub>S/N<sub>2</sub> and H<sub>2</sub>S/CH<sub>4</sub> pairs seems impossible, since there are no data for liquid membranes. From the presented values of mass transport characteristics of the combined system, it is evident that the permeability of that system is many times lower than that of a membrane, especially exposed to hydrogen sulfide. At the same time, the selectivity of the system increases significantly, which is obviously associated with the use of an absorption solution.

### 3.3. Performance test of the developed membrane-assisted gas absorption unit

#### 3.1.1. Separation of the model gas mixture

The efficiency of the proposed technique during the natural gas processing was evaluated on the example of two gas mixtures: three-component, containing methane, carbon dioxide and xenon in the ratio 94.5/5.35/0.15 vol.% and an eight-component mixture containing methane, ethane, carbon dioxide, propane, nitrogen, butane, hydrogen sulfide and xenon at a ratio of 75.67/7.41/5.396/4.534/3.013/2.469/1.389/0.113 vol.%. A 30 wt.% aqueous solution of amino alcohol - methyldiethanolamine was used as an absorbent. The results obtained for the separation process of the three-component gas mixture are shown in Figures 6 and 7. Fig. 6 contains data on the dependences of the content of the components of the ternary gas mixture in the retentate flow on the stage-cut. Fig. 7 shows the dependences of methane and carbon dioxide content in the permeate flow on the stage-cut. The dependence of xenon content in the permeate flow on the stage-cut is not shown, as in the whole range of stage-cut value its content was below the detection limit of the gas chromatograph equipped with a thermal conductivity detector with increased sensitivity. This allows us to conclude that the xenon content in the permeate stream did not exceed 10 ppm.

From the presented dependence of methane concentration on the stage-cut (Fig. 6a) it can be seen that when the process is carried out with the minimum value of the stage-cut,

no change in the composition of the separated mixture is observed. So, methane concentration in a retentate stream is 94.59 vol.% thus, that its initial concentration in a mix was equal 94.5 vol.%. However, maximum achieved concentration of this component in the retentate flow is 98.8 vol.%. It is evident from the presented dependence that the growth of stage-cut is accompanied by a significant growth of methane content in the retentate flow. Such dependence is explained by the fact that methane is a low-soluble component in the used absorption system, as well as by the fact that the membrane permeability value for this component is significantly lower than the same value for carbon dioxide. Since the stage-cut is determined by the ratio of the permeate flow rate to the feed flow rate, increasing the stage-cut means increasing the permeate flow rate (if the feed flow rate is constant). Thus, when the stage-cut increases, a more soluble component - carbon dioxide permeates the combined membrane-absorbent system, which allows to obtain more concentrated methane in the retentate flow.

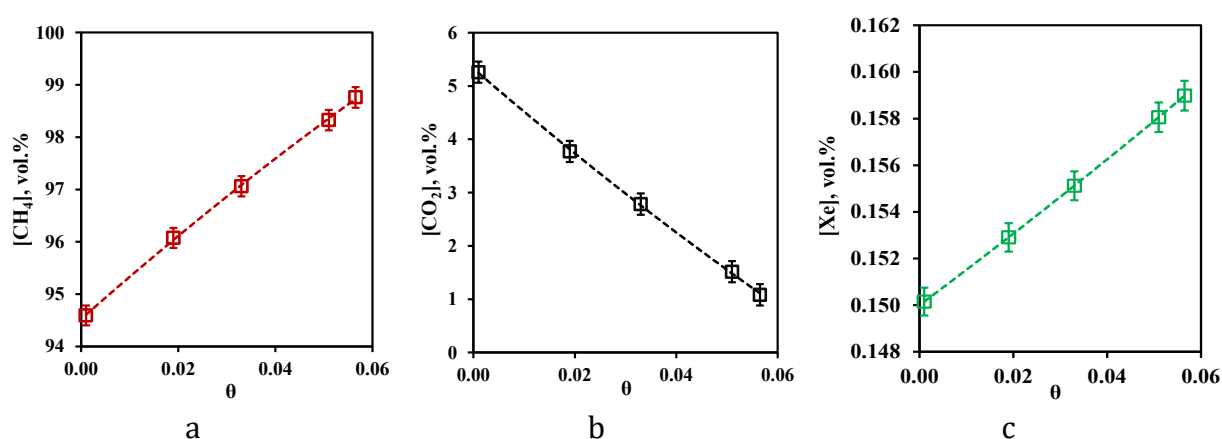


**Figure 6** Dependence of methane (a), carbon dioxide (b) and xenon (c) content in the retentate flow on the stage-cut during the separation of a three-component gas mixture using a membrane-assisted gas absorption unit

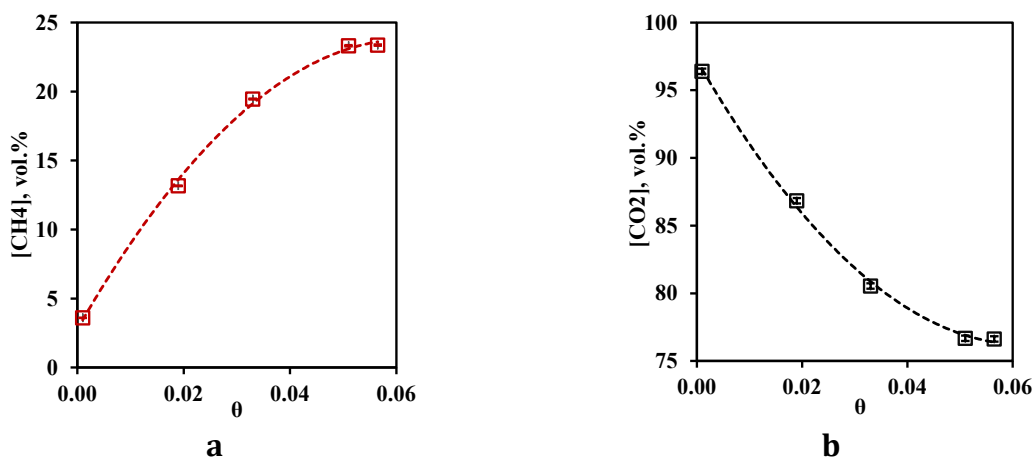
Dependence of carbon dioxide content in the retentate flow on the stage-cut, presented in Fig. 6b is in good agreement with the conclusions described above. It can be seen that the growth of the stage-cut is accompanied by a sharp decrease in carbon dioxide content in the retentate stream. So, at the minimum value of the stage-cut, the concentration of carbon dioxide is equal to 5.26 vol.% at its initial content of 5.35 vol.%. Thus, carrying out the process at the maximum value of stage-cut allows to lower concentration of carbon dioxide in the retentate flow to 1.08 vol.%. Such dependence is explained by the fact that carbon dioxide is soluble in the used absorption system, and its efficient removal from the system at a higher flow rate of permeate allows to remove most of it from the separated gas mixture.

Figure 6c shows the dependence of xenon content in the retentate flow on the stage-cut. From the obtained curve describing this dependence it can be seen that the growth of the stage-cut value is accompanied by slow increase in xenon concentration in the withdrawn flow. In this case, carrying out the process at the lowest value of the stage-cut maintain the initial concentration of xenon. However, a further increase in the stage-cut practically does not affect the change in xenon concentration in the retentate flow. This dependence is explained by two factors: the ability of xenon to dissolve in water, low permeability of the membrane used and relatively large kinetic diameter of the xenon molecule. Thus, the reduction of xenon concentration in the retentate flow compared to its content in feed is most likely due to the fact that some of it is dissolved in the water contained in the liquid absorbent. At the same time, low membrane permeability to this



component and large size of the molecule do not allow xenon to permeate through the combined membrane-absorbent system. This explains the fact that in the permeate stream the xenon content was below the GC detection limit. The increase in the xenon concentration observed with the increase of the stage-cut is due to the fact that the solubility limit for this component is reached in the membrane-absorber module, which, at the same time, leads to some loss of this component in the absorbent. However, the xenon is not permeated to the submembrane space, which indicates that these losses are not irreversible. Thus, regeneration of the absorbent used will allow the extraction of the dissolved xenon. This effect should be taken into account in further optimization of the proposed technique.

Figure 7a shows the dependence of methane concentration in the permeate flow on the stage-cut during separation of a three-component gas mixture. From the presented curve it is seen that the growth of the stage-cut is accompanied by an increase in the methane concentration in the permeate stream. So, at the lowest value of the stage-cut, the methane concentration is equal to 3.6 vol.%, and at the stage-cut value of 0.05 and 0.06, the methane content in the permeate stream is 23.32 and 23.37 vol.%, respectively. It is seen that a change in the stage-cut from 0.05 to 0.06, is not accompanied by a significant change in the concentration of methane in the permeate stream, while the change in the stage-cut from 0.02 to 0.03 causes a sharp increase in the methane content in this stream. The dependence obtained for the permeate flow agrees well with the data obtained for the retentate flow. Thus, an increase in the stage-cut and, consequently, an increase in the permeate flow rate leads to an increase in the fraction of methane permeating through the combined membrane-absorbent system. Since methane is practically insoluble in the absorbent used, its transfer through this system is most likely caused by diffusion processes. Such an effect requires an additional study aimed at determining the diffusion coefficients of the gases included in the mixtures.



**Figure 7** Dependence of methane content in the permeate flow on the stage-cut during the separation of a three-component gas mixture using a membrane-assisted gas absorption unit

Figure 7b illustrates the dependence of carbon dioxide content in the permeate flow on the stage-cut, at which the separation process in membrane-assisted gas absorption unit is realized.

From the curve shown in the figure is seen that increase of the stage-cut in the whole observed range is accompanied by change of a content of carbon dioxide from 96.4 to 76.6 vol.%. At the same time, the concentration of carbon dioxide does not fall below 76.6 vol.%, which allows to make a conclusion about high efficiency of the proposed technique, because



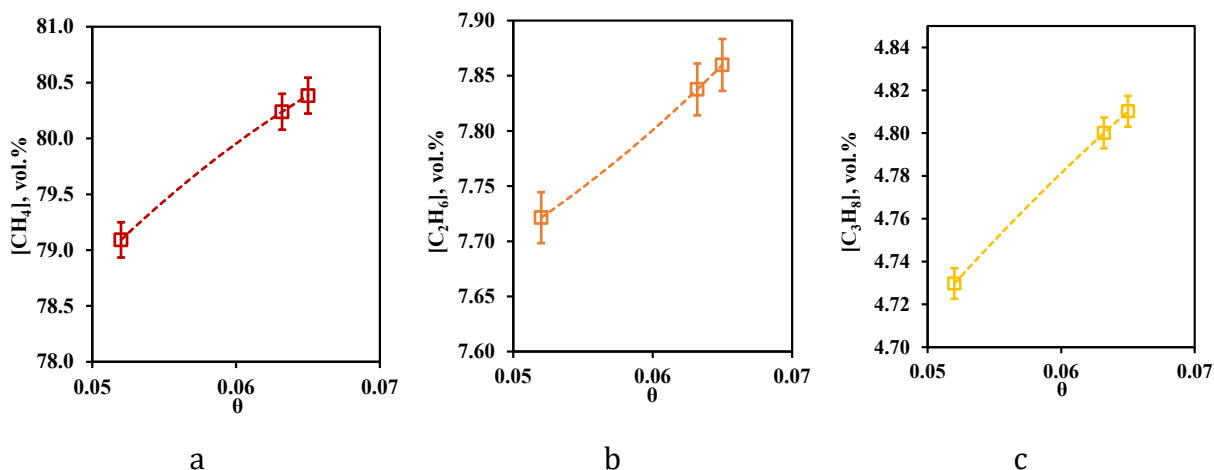
the conventional membrane gas separation rarely allows to obtain a carbon dioxide concentrate of more than 50 - 65 vol.% in one stage even when using a highly selective membrane (Merkel et al., 2010).

As a result of the cumulative analysis of the obtained results on the example of separation of a three-component gas mixture, it may be concluded that the proposed technique is promising for the task of removing acid gases from the natural gas flow. Thus, the maximum purity of methane, withdrawn in the form of retentate flow is 98.8 vol.%, at its same content in the permeate flow at a level  $\sim 24$  vol.%. To reduce methane losses in the permeate stream, optimization of the process is required, aimed at selection of the most effective absorbent solution. Its selective adsorption will reduce the transfer of methane into the submembrane space.

### 3.1.2 Separation of quasi-real mixture

For more detailed and approbation of the proposed technique, a similar study for an eight-component gas mixture containing methane, ethane, carbon dioxide, propane, nitrogen, butane, hydrogen sulfide and xenon in the ratio: 75.677/7.41/5.396/4.534/3.013/2.469/1.389/0.113 mol% was conducted. Figures 8, 9 show the results of quasi-real gas mixture separation. Figure 8 shows data on the composition of the retentate stream as a function of stage-cut. Figure 9 presents data on the composition of the permeate stream from stage-cut. Similarly to the previous case, data on xenon in both streams are not given due to the fact that its content is below the detection limit of the gas chromatograph, even though a thermal conductivity detector with increased sensitivity was used. Based on this, it can be concluded that the xenon content in the permeate does not exceed 10 ppm.

In Fig. 8a the dependence of methane concentration in the retentate flow on the stage-cut is presented. From the presented curve it is visible that change of methane content is in a range from 79.1 to 80.4 vol.% that speaks about insignificant change of this value from the stage-cut at which process is realized. Given the initial content of this component in the mixture (75.677 vol.%), it can be concluded that the membrane-assisted gas absorption process contributes to an insignificant concentration of methane in the withdrawn flow. In this case, an increase in the stage-cut is accompanied by an increase in the methane concentration value, which agrees well with the data obtained earlier for the three-component gas mixture. The obtained dependence is explained by the fact that the growth of the stage-cut is caused by an increase in the permeate flow rate. This, in turn, contributes to a more efficient removal of soluble components to the permeate side. Since methane is practically insoluble in the selected absorbent, its buildup in the retentate flow occurs.



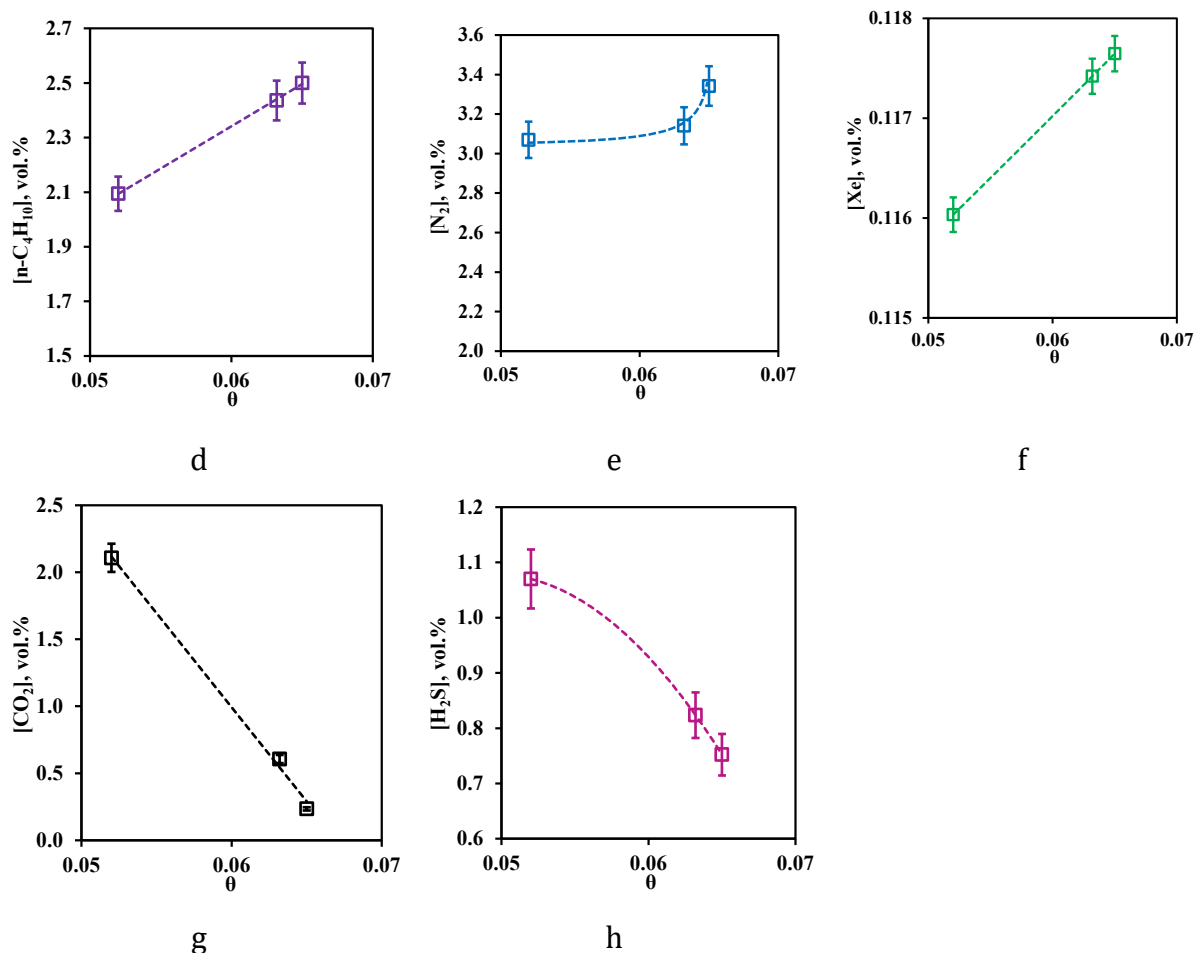


**Figure 8** - Dependence of methane (a), ethane (b), propane(c),n- butane (d), nitrogen (e), xenon (f), carbon dioxide (g) and hydrogen sulfide (h) content in the retentate flow on the stage-cut during the separation of an eight-component gas mixture using a membrane-assisted gas absorption unit

Figure 8b shows the dependence of ethane content in the retentate flow on the stage-cut, at which the gas separation process is realized. From the presented dependence it can be seen that the concentration of ethane, as well as in the case of methane, practically does not depend on the value of the stage-cut. Thus, as the stage-cut growth, the content of this component in the retentate stream is observed very insignificantly, namely, the ethane concentration increases from 7.72 to 7.86 vol. % when changing the stage-cut from 0.05 to 0.065. Since ethane also is a low-soluble component, its concentration depends on the gas flow rate passing through the combined membrane-absorbent system insignificantly. Comparing the concentration of ethane in the feed flow with its initial content in the mixture (7.41 vol.%), we can see that there is an insignificant concentration of this component.

Figure 8c shows the dependence of propane content in the retentate stream on the stage-cut. From this curve it can be seen that the tendency described above for other hydrocarbons is also observed for propane. So, at the stage-cut value of 0.05 the propane content in the permeate stream is at a level of 4.73 vol.%. At the maximum value of the stage-cut (0.065) its concentration is 4.81 vol.%. Here it is necessary to note, that as a result of carrying out of process even at the lowest value of the stage-cut, which promotes the least concentration of hardly permeable and low-soluble components, the growth of the propane content equal to 0.2 vol.%, in comparison with its initial content is observed.

Figure 8d illustrates the dependence of n-butane concentration in the retentate flow on the stage-cut. From the obtained dependence it can be seen that in this case, the change of stage-cut causes more pronounced change in the content of this component in the retentate flow than in the case of ethane and propane. Thus, carrying out the process at the stage-cut equal to 0.05, a decrease in the n-butane concentration value ( $\sim 2.1$  vol.%) is observed in comparison with its initial content in the mixture (2.469 vol.%). However, an increase in the stage-cut to 0.065 is accompanied by an increase in the n-butane concentration to 2.5 vol.%, which is equal to its initial content. Thus, the cumulative analysis of dependencies of concentrations of hydrocarbons on value of the stage-cut shows that on all these components insignificant concentration change is observed at carrying out the process with the stage-cut value  $\geq 0.06$ . Thus, application of a hybrid method - membrane-assisted gas absorption allows to concentrate these components in the retentate stream.

Figure 8e shows the dependence of nitrogen content in the retentate flow on the stage-cut. The obtained dependence shows that the nitrogen content in the captured retentate stream does not depend on the value of the stage-cut, at which the gas separation process is implemented. Thus, the concentration of nitrogen in the whole considered range of stage-cut values varies from 3.1 to 3.34 vol.%. At the same time, comparing the achieved nitrogen concentration with its initial content in the separated gas mixture, it can be seen that its content increased by 0.33 vol.%. Thus, we can conclude that the implementation of the membrane-assisted gas absorption process allows to slightly concentrate nitrogen, which is also a low-soluble component unable to permeate and concentrate on the permeate side.

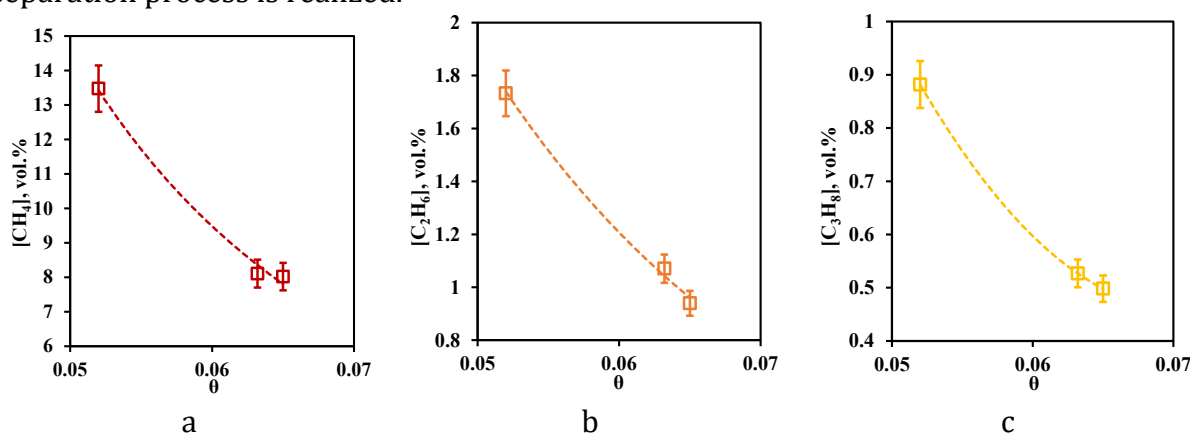
Figure 8f illustrates the dependence of xenon content in the retentate flow on the stage-cut value. In general, for xenon a dependence similar to nitrogen is observed. In the whole considered range of the stage-cut, the xenon concentration value varies from 0.116 to 0.117 vol.%. However, there is a weak tendency of increase in xenon concentration with increase in the stage-cut, at which gas separation process is realized. Thus, at the stage-cut equal to 0.05, xenon concentration is equal to 0.116 vol.%, and at the stage-cut equal to 0.065, xenon concentration decreases to 0.117 vol.%. As is seen, there is a linear dependence of Xe content on stage-cut. The dependence obtained for the eight-component mixture is in well agreement with the same dependence obtained for the ternary mixture. Despite the fact that xenon is able to dissolve in the water contained in the liquid absorbent used, this does not occur in the presence of other components (nitrogen, ethane, propane, n-butane, hydrogen sulfide) that are absent in the triple mixture. Most likely, this dependence can be explained by a specific sorption realized in the presence of an even more soluble gas - hydrogen sulfide. Presumably, the solubility limit is reached in the membrane-assisted gas absorption unit, which does not allow xenon to sorb in a liquid saturated with more soluble components - carbon dioxide and hydrogen sulfide.

Figure 8g shows the dependence of carbon dioxide content in the retentate flow on the stage-cut. The obtained dependence shows that an increase in the stage-cut is accompanied by a decrease in carbon dioxide content in the retentate stream, withdrawn from the membrane-assisted gas absorption module. Thus, the maximum concentration of carbon dioxide is 2.1 vol.% at the stage-cut equal to 0.05. Performing the separation process at the stage-cut of 0.065, the carbon dioxide content decreases to 0.23 vol.%. At the same time, there is a significant decrease in the concentration of carbon dioxide compared with its initial content in the mixture (5.396 vol.%). Thus, at the stage-cut of 0.05, the concentration of carbon dioxide decreases by 3.3 vol.%, and at the process stage-cut value of 0.065, the concentration of carbon dioxide decreases by 5.17 vol.%. The obtained dependence is explained by the fact that carbon dioxide, firstly, is well dissolved in the used liquid absorbent, and secondly, the membrane is characterized by the highest permeability by this

component (among the components of the mixture). Thus, in the process under consideration, carbon dioxide is able to dissolve effectively in the liquid absorbent layer and move into the submembrane space of the membrane-assisted gas absorption unit.

In figure 8h the dependence of hydrogen sulfide concentration on the stage-cut value, at which the separation process is carried out, is presented. From the received curve it is visible that growth of the stage-cut is accompanied by decrease in hydrogen sulfide content in a retentate stream. So, at the stage-cut equal to 0.05 the hydrogen sulfide concentration makes 1.07 vol.%, and at the stage-cut equal to 0.065 the hydrogen sulfide concentration is equal to 0.75 vol.%. Thus, as a result of this process decrease in the hydrogen sulfide content in comparison with its initial concentration in a mix from 0.32 to 0.64 vol.% is observed. Like in the case of carbon dioxide, the obtained dependence is explained by the absorbent ability to effectively dissolve this component and relatively high membrane permeance to hydrogen sulfide, which provides effective transfer of this gas to the permeate side. Thus, implementation of the process at the stage-cut value equal to 0.65, the gas stream withdrawn as retentate consists of methane, ethane, carbon dioxide, propane, nitrogen, n-butane, hydrogen sulfide and xenon in the ratio 80.39/7.86/0.23/4.81/3.34/2.50/0.75/0.12 vol.%, which corresponds to an increase in the concentration of all components except impurities of acid gases, and, equally importantly, preservation and a slight increase in xenon content.

Analyzing the composition of permeate flow at different values of the stage-cut it is seen that the dependences of concentrations of methane, ethane, propane, n-butane and nitrogen (Figure 9) on the stage-cut form the curves of similar character and similar in intensity of concentration decrease, accompanying the increase of the stage-cut value. So, in process of increase in the stage-cut from 0.05 to 0.065, decrease in concentration of these components from 54.2 to 66.3 % from the value received for the stage-cut equal to 0.05 is observed. In absolute values this corresponds to the following values: 8.02, 0.94, 0.49, 0.23, 1.06 vol.% for methane, ethane, propane, n-butane, and nitrogen when the process is conducted with the stage-cut equal to 0.065. An explanation of the obtained dependencies is given above. All these components are low-soluble components of a mixture that causes low efficiency of their transfer through the combined membrane-absorbent system, and, as consequence, their low content in a permeate stream that corresponds to small losses on these components even at high value of the stage-cut at which the considered gas separation process is realized.



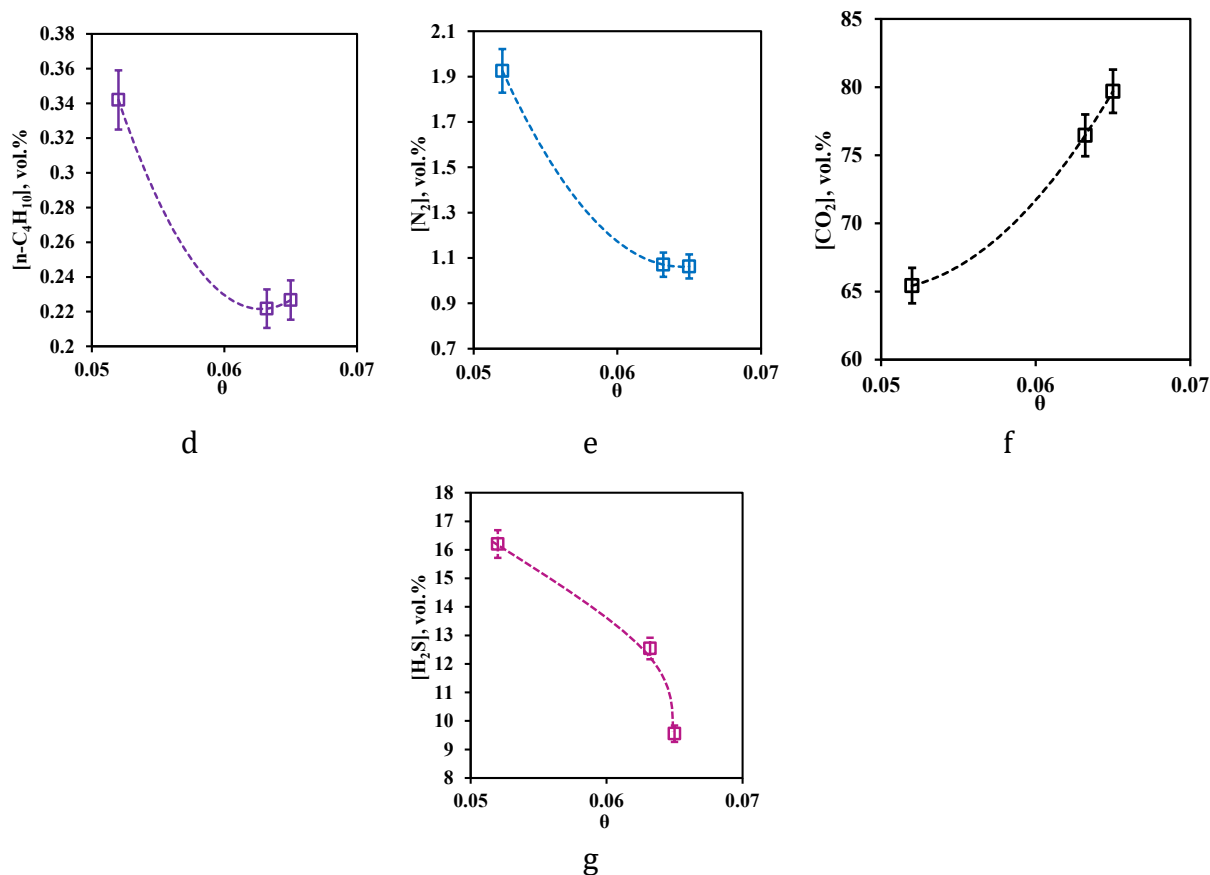


**Figure 9** Dependence of methane (a), ethane (b), propane(c),n- butane (d), nitrogen (e), carbon dioxide (f) and hydrogen sulfide (g) content in the permeate flow on the stage-cut during the separation of an eight-component gas mixture using a membrane-assisted gas absorption unit

Fig. 9f and 9g show the dependences of concentration of impurities of acid gases - carbon dioxide and hydrogen sulfide in permeate flow on the stage-cut. From the presented curves it is seen that the character of these dependences is opposite, but the values of concentrations of these components are high. So, the concentration of carbon dioxide is in a range 65.43 - 79.7 vol.%, and hydrogen sulfide content in the permeate stream is 9.55 - 16.21 vol.%. For carbon dioxide there is a significant growth of its concentration caused by growth of the stage-cut. At transition of a value of the stage-cut from 0.052 to 0.06 the concentration of carbon dioxide increases by 11 vol.% and at increase of the cut to 0.065 concentration of carbon dioxide increases by 14.27 vol.%. Decrease in hydrogen sulfide concentration in a permeate stream caused by increase of the stage-cut is less intensive and makes 3.66 and 2.99 vol.% at the same step increase of the stage-cut value. Thus, performing the membrane-assisted gas absorption process at the stage-cut equal to 0.065 (which corresponds to the most effective concentration of hydrocarbons in the retentate stream) allows to receive a permeate stream enriched with acid gases. The composition of such flow corresponds to the following proportion of methane, ethane, carbon dioxide, propane, nitrogen, n-butane, hydrogen sulfide 8.02/0.94/79.7/0.5/1.06/0.23/9.55 vol.%.

The ultimate efficiency of considered process represented as removed amount of acid gases is 96 and 61 % of carbon dioxide and hydrogen sulfide, respectively. Under the same conditions the hydrocarbons losses were up to 0.95 %. In this way, the residual sum of acid gases content may be lowered to 0.99 vol.% from 6.79 vol.% in one stage using the heat-free hybrid membrane-assisted gas absorption technique maintaining suitable recovery rate of methane, ethane, propane and n-butane. The content of acid gases in processed gas

stream meets the limitations indicated in Russian Government Standard (GOST 5542-2022). Nevertheless, the overall efficiency of the process may be enhanced using the specific absorption agents with aqueous amino alcohol solutions.

#### 4. Conclusions

This paper presents a continuation of the development and investigation of the MAGA method. The possibility of improving the efficiency of the system by optimising the cell configuration was discussed. The optimisation of the configuration consists in the use of two types of hollow fibres, which reduces the ratio between the absorbent volume and the membrane area. The complexity of approach to evaluation of membrane-assisted gas absorption process efficiency is stated by the consideration of two gas mixes: ternary model mix and quasi-real natural gas. As a result of the present experimental study of the novel heat-free process in natural gas sweetening application, it was shown that sum of acid gases content may be lowered to less than 1 vol.% in one stage in a continuous mode without any of pumping gear and specific absorbent regeneration step. The composition of product stream is methane, ethane, carbon dioxide, propane, nitrogen, n-butane, hydrogen sulfide and xenon in the ratio 80.39/7.86/0.23/4.81/3.34/2.50/0.75/0.12 vol.%. In this way, the ultimate efficiency of considered process represented as removed amount of acid gases is 96 and 61 % of carbon dioxide and hydrogen sulfide, respectively. Taking into account many variations of natural gas composition, for example, the higher acid gases content, the membrane-assisted gas absorption process may be tuned by increasing the membrane area, absorbent composition and its content to achieve the desirable result. Moreover, typical requirement for CO<sub>2</sub> content in natural gas supplied to pipeline is less than 2 %, meanwhile the proposed technique allows to decrease it to 0.23 % with minimal loss of valuable hydrocarbons. Nevertheless, the overall efficiency of the process may be enhanced using the specific absorption agents with aqueous amino alcohol solutions. For example, ionic liquids, piperazine, and other alkanolamines, are used as additives that increase the sorption capacity of such solutions. The further study will be devoted to the appliance of novel absorbent systems, based on «green» and cheap ionic liquids, which allow to increase the absorption capacity of alkanolamine aqueous solutions.

#### Acknowledgments

The main part of the study was supported by the Russian Science Foundation (project no. 22-79-10222). The analytical support was funded by Ministry of Science and Education of the Russian Federation within the framework of the scientific project of the laboratory «Laboratory of Electronic Grade Substances Technologies», project No. FSSM2022-0005.

#### Conflict of Interest

The authors declare no conflicts of interest.

#### References

- Atlaskin, A.A., Kryuchkov, S.S., Smorodin, K.A., Markov, A.N., Kazarina, O. V., Zarubin, D.M., Atlaskina, M.E., Vorotyntsev, A. V., Nyuchev, A. V., Petukhov, A.N., Vorotyntsev, I. V., 2021a. Towards the potential of trihexyltetradecylphosphonium indazolidine with aprotic heterocyclic ionic liquid as an efficient absorbent for membrane-assisted gas absorption technique for acid gas removal applications. *Sep Purif Technol* 257, 117835. <https://doi.org/10.1016/J.SEPPUR.2020.117835>

- Atlaskin, A.A., Kryuchkov, S.S., Smorodin, K.A., Markov, A.N., Kazarina, O. V., Zarubin, D.M., Atlaskina, M.E., Vorotyntsev, A. V., Nyuchev, A. V., Petukhov, A.N., Vorotyntsev, I. V., 2021b. Towards the potential of trihexyltetradecylphosphonium indazolidine with aprotic heterocyclic ionic liquid as an efficient absorbent for membrane-assisted gas absorption technique for acid gas removal applications. *Sep Purif Technol* 257, 117835. <https://doi.org/10.1016/J.SEPPUR.2020.117835>
- Atlaskin, A.A., Kryuchkov, S.S., Yanbikov, N.R., Smorodin, K.A., Petukhov, A.N., Trubyanov, M.M., Vorotyntsev, V.M., Vorotyntsev, I. V., 2020a. Comprehensive experimental study of acid gases removal process by membrane-assisted gas absorption using imidazolium ionic liquids solutions absorbent. *Sep Purif Technol* 239, 116578. <https://doi.org/10.1016/J.SEPPUR.2020.116578>
- Atlaskin, A.A., Kryuchkov, S.S., Yanbikov, N.R., Smorodin, K.A., Petukhov, A.N., Trubyanov, M.M., Vorotyntsev, V.M., Vorotyntsev, I. V., 2020b. Comprehensive experimental study of acid gases removal process by membrane-assisted gas absorption using imidazolium ionic liquids solutions absorbent. *Sep Purif Technol* 239, 116578. <https://doi.org/10.1016/J.SEPPUR.2020.116578>
- Bashir, Z., Lock, S.S.M., Hira, N. e., Ilyas, S.U., Lim, L.G., Lock, I.S.M., Yiin, C.L., Darban, M.A., 2024. A review on recent advances of cellulose acetate membranes for gas separation. *RSC Adv* 14, 19560–19580. <https://doi.org/10.1039/D4RA01315H>
- Bello, M.O., Solarin, S.A., 2022. Searching for sustainable electricity generation: The possibility of substituting coal and natural gas with clean energy. *Energy and Environment* 33, 64–84. [https://doi.org/10.1177/0958305X20985253/ASSET/IMAGES/LARGE/10.1177\\_0958305X20985253-FIG1.JPEG](https://doi.org/10.1177/0958305X20985253/ASSET/IMAGES/LARGE/10.1177_0958305X20985253-FIG1.JPEG)
- Berchiche, A., Guenoune, M., Belaadi, S., Léonard, G., 2023. Optimal Energy Integration and Off-Design Analysis of an Amine-Based Natural Gas Sweetening Unit. *Applied Sciences* 2023, Vol. 13, Page 6559 13, 6559. <https://doi.org/10.3390/APP13116559>
- Darani, N.S., Behbahani, R.M., Shahebrahimi, Y., Asadi, A., Mohammadi, A.H., 2021. Simulation and optimization of the acid gas absorption process by an aqueous diethanolamine solution in a natural gas sweetening unit. *ACS Omega* 6, 12072–12080. [https://doi.org/10.1021/ACSOMEGA.1C00744/ASSET/IMAGES/MEDIUM/AO1C00744\\_M009.GIF](https://doi.org/10.1021/ACSOMEGA.1C00744/ASSET/IMAGES/MEDIUM/AO1C00744_M009.GIF)
- Davarpanah, E., Hernández, S., Latini, G., Pirri, C.F., Bocchini, S., 2020. Enhanced CO<sub>2</sub> Absorption in Organic Solutions of Biobased Ionic Liquids. *Adv Sustain Syst* 4, 1900067. <https://doi.org/10.1002/ADSU.201900067>
- Dawodu, O.F., Meisen, A., 1994. Solubility of Carbon Dioxide in Aqueous Mixtures of Alkanolamines. *J Chem Eng Data* 39, 548–552. [https://doi.org/10.1021/JE00015A034/ASSET/JE00015A034.FP.PNG\\_V03](https://doi.org/10.1021/JE00015A034/ASSET/JE00015A034.FP.PNG_V03)
- Ellaf, A., Ali Ammar Taqvi, S., Zaeem, D., Siddiqui, F.U.H., Kazmi, B., Idris, A., Alshgari, R.A., Mushab, M.S.S., 2023. Energy, exergy, economic, environment, exergo-environment based assessment of amine-based hybrid solvents for natural gas sweetening. *Chemosphere* 313, 137426. <https://doi.org/10.1016/J.CHEMOSPHERE.2022.137426>
- Friess, K., Izák, P., Kárászová, M., Pasichnyk, M., Lanč, M., Nikolaeva, D., Luis, P., Jansen, J.C., 2021. A Review on Ionic Liquid Gas Separation Membranes. *Membranes* 2021, Vol. 11, Page 97 11, 97. <https://doi.org/10.3390/MEMBRANES11020097>



- Fu, D., Zhang, P., Mi, C.L., 2016a. Effects of concentration and viscosity on the absorption of CO<sub>2</sub> in [N1111][Gly] promoted MDEA (methyldiethanolamine) aqueous solution. *Energy* 101, 288–295. <https://doi.org/10.1016/J.ENERGY.2016.02.052>
- Fu, D., Zhang, P., Wang, L.M., 2016b. Absorption performance of CO<sub>2</sub> in high concentrated [Bmim][Lys]-MDEA aqueous solution. *Energy* 113, 1–8. <https://doi.org/10.1016/J.ENERGY.2016.07.049>
- Ghasem, N., 2020. CO<sub>2</sub> removal from natural gas. *Advances in Carbon Capture: Methods, Technologies and Applications* 479–501. <https://doi.org/10.1016/B978-0-12-819657-1.00021-9>
- Godin, J., Liu, W., Ren, S., Xu, C.C., 2021. Advances in recovery and utilization of carbon dioxide: A brief review. *J Environ Chem Eng* 9, 105644. <https://doi.org/10.1016/J.JECE.2021.105644>
- GOST 5542-2022. Natural gas for industrial and municipal purposes. Technical conditions [WWW Document], n.d. URL <https://internet-law.ru/gosts/gost/77776/> (accessed 8.14.24).
- Hadri, N.E.L., Quang, D.V., Abu-Zahra, M.R.M., 2015a. Study of Novel Solvent for CO<sub>2</sub> Post-combustion Capture. *Energy Procedia* 75, 2268–2286. <https://doi.org/10.1016/J.EGYPRO.2015.07.414>
- Hadri, N.E.L., Quang, D.V., Abu-Zahra, M.R.M., 2015b. Study of Novel Solvent for CO<sub>2</sub> Post-combustion Capture. *Energy Procedia* 75, 2268–2286. <https://doi.org/10.1016/J.EGYPRO.2015.07.414>
- Hazarika, G., Ingole, P.G., 2024. Polymer-based hollow fiber membranes: A modern trend in gas separation technologies. *Mater Today Chem* 38, 102109. <https://doi.org/10.1016/J.MTCHEM.2024.102109>
- Ibrahim, A.Y., Ashour, F.H., Gadalla, M.A., Farouq, R., 2022. Exergy study of amine regeneration unit for diethanolamine used in refining gas sweetening: A real start-up plant. *Alexandria Engineering Journal* 61, 101–112. <https://doi.org/10.1016/J.AEJ.2021.04.085>
- Jamal, A., Meisen, A., Jim Lim, C., 2006. Kinetics of carbon dioxide absorption and desorption in aqueous alkanolamine solutions using a novel hemispherical contactor—I. Experimental apparatus and mathematical modeling. *Chem Eng Sci* 61, 6571–6589. <https://doi.org/10.1016/J.CES.2006.04.046>
- Jana, A., Modi, A., 2024. Recent progress on functional polymeric membranes for CO<sub>2</sub> separation from flue gases: A review. *Carbon Capture Science & Technology* 11, 100204. <https://doi.org/10.1016/J.CCST.2024.100204>
- Jou, F. -Y., Mather, A.E., Otto, F.D., 1995. The solubility of CO<sub>2</sub> in a 30 mass percent monoethanolamine solution. *Can J Chem Eng* 73, 140–147. <https://doi.org/10.1002/CJCE.5450730116>
- Karamah, E.F., Arbi, D.S., Bagas, I., Kartohardjono, S., 2021. Hollow Fiber Membrane Modules for NO<sub>x</sub> Removal using a Mixture of NaClO<sub>3</sub> and NaOH Solutions in the Shell Side as Absorbents. *International Journal of Technology* 12, 690–699. <https://doi.org/10.14716/IJTECH.V12I4.4408>
- Kartohardjono, S., Karamah, E.F., Talenta, G.N., Ghazali, T.A., Lau, W.J., 2023. The Simultaneously Removal of NO<sub>x</sub> and SO<sub>2</sub> Processes through a Polysulfone Hollow

Fiber Membrane Module. *International Journal of Technology* 14, 576–583.  
<https://doi.org/10.14716/IJTECH.V14I3.5544>

Khan, A.U., Hazaraimi, M.H., Othman, M.H.D., Younas, M., Karim, Z.A., Tai, Z.S., Samuel, O., Puteh, M.H., Kurniawan, T.A., Wong, K.Y., Yoshida, N., 2024. A comprehensive review on dual-layer organic hollow fiber membranes fabrication via co-extrusion: Mechanistic insights, water treatment and gas separation applications. *J Environ Chem Eng* 12, 112434. <https://doi.org/10.1016/J.JECE.2024.112434>

Khan, I.U., Othman, M.H.D., Jilani, A., 2021. High Performance Membrane for Natural Gas Sweetening Plants. *Advances in Science, Technology and Innovation* 59–72.  
[https://doi.org/10.1007/978-3-030-41295-1\\_5/TABLES/6](https://doi.org/10.1007/978-3-030-41295-1_5/TABLES/6)

Kryuchkov, S., Smorodin, K., Stepakova, A., Atlaskin, A., Tsivkovsky, N., Atlaskina, M., Tolmacheva, M., Kazarina, O., Petukhov, A., Vorotyntsev, A., Vorotyntsev, I., 2024. Membrane Air Separation Process Simulation: Insight in Modelling Approach Based on Ideal and Mixed Permeance Values. *International Journal of Technology* 15, 1218.  
<https://doi.org/10.14716/IJTECH.V15I5.6987>

Kryuchkov, S.S., Petukhov, A.N., Atlaskin, A.A., 2021. Experimental Evaluation of the Membrane-Assisted Gas Absorption Technique Efficiency Using an Aqueous Solution Of PEG-400 for the Ammonia Capture. *IOP Conf Ser Earth Environ Sci* 666, 052071.  
<https://doi.org/10.1088/1755-1315/666/5/052071>

Lei, L., Bai, L., Lindbråthen, A., Pan, F., Zhang, X., He, X., 2020. Carbon membranes for CO<sub>2</sub> removal: Status and perspectives from materials to processes. *Chemical Engineering Journal* 401, 126084. <https://doi.org/10.1016/J.CEJ.2020.126084>

Liang, Y., Kleijn, R., Tukker, A., van der Voet, E., 2022. Material requirements for low-carbon energy technologies: A quantitative review. *Renewable and Sustainable Energy Reviews* 161, 112334. <https://doi.org/10.1016/J.RSER.2022.112334>

Litvinenko, V., 2020. The Role of Hydrocarbons in the Global Energy Agenda: The Focus on Liquefied Natural Gas. *Resources* 2020, Vol. 9, Page 59 9, 59.  
<https://doi.org/10.3390/RESOURCES9050059>

Liu, G., Zhu, L., Cao, W., Liu, H., He, Y., 2021. New Technique Integrating Hydrate-Based Gas Separation and Chemical Absorption for the Sweetening of Natural Gas with High H<sub>2</sub>S and CO<sub>2</sub> Contents. *ACS Omega* 6, 26180–26190.  
[https://doi.org/10.1021/ACSOMEGA.1C03165/ASSET/IMAGES/LARGE/AO1C03165\\_0010.JPEG](https://doi.org/10.1021/ACSOMEGA.1C03165/ASSET/IMAGES/LARGE/AO1C03165_0010.JPEG)

Liu, Y., Chen, Z., Qiu, W., Liu, G., Eddaoudi, M., Koros, W.J., 2021a. Penetrant competition and plasticization in membranes: How negatives can be positives in natural gas sweetening. *J Memb Sci* 627, 119201.  
<https://doi.org/10.1016/J.MEMSCI.2021.119201>

Liu, Y., Liu, Z., Kraftschik, B.E., Babu, V.P., Bhuwania, N., Chinn, D., Koros, W.J., 2021b. Natural gas sweetening using TEGMC polyimide hollow fiber membranes. *J Memb Sci* 632, 119361. <https://doi.org/10.1016/J.MEMSCI.2021.119361>

Liu, Y., Liu, Z., Morisato, A., Bhuwania, N., Chinn, D., Koros, W.J., 2020. Natural gas sweetening using a cellulose triacetate hollow fiber membrane illustrating controlled plasticization benefits. *J Memb Sci* 601, 117910.  
<https://doi.org/10.1016/J.MEMSCI.2020.117910>

- Mahi, M.R., Mokbel, I., Negadi, L., Dergal, F., Jose, J., 2019. Experimental solubility of carbon dioxide in monoethanolamine, or diethanolamine or N-methyldiethanolamine (30 wt%) dissolved in deep eutectic solvent (choline chloride and ethylene glycol solution). *J Mol Liq* 289, 111062. <https://doi.org/10.1016/J.MOLLIQ.2019.111062>
- Makertihartha, I.G.B.N., Kencana, K.S., Dwiputra, T.R., Khoiruddin, K., Lugito, G., Mukti, R.R., Wenten, I.G., 2022. SAPO-34 zeotype membrane for gas sweetening. *Reviews in Chemical Engineering* 38, 431–450. <https://doi.org/10.1515/REVCE-2019-0086/XML>
- Merkel, T.C., Lin, H., Wei, X., Baker, R., 2010. Power plant post-combustion carbon dioxide capture: An opportunity for membranes. *J Memb Sci* 359, 126–139. <https://doi.org/10.1016/J.MEMSCI.2009.10.041>
- Nasteka, V.I., 1996. New technologies of refinery of high-sulfur and gas condensate. Moscow: Nedra, pp 1-106.
- Niu, Z., He, N., Yao, Y., Ma, A., Zhang, E., Cheng, L., Li, Y., Lu, X., 2024. Mixed matrix membranes for gas separations: A review. *Chemical Engineering Journal* 494, 152912. <https://doi.org/10.1016/J.CEJ.2024.152912>
- Østergaard, P.A., Duic, N., Noorollahi, Y., Mikulcic, H., Kalogirou, S., 2020. Sustainable development using renewable energy technology. *Renew Energy* 146, 2430–2437. <https://doi.org/10.1016/J.RENENE.2019.08.094>
- Otvagina, K. V., Penkova, A. V., Dmitrenko, M.E., Kuzminova, A.I., Sazanova, T.S., Vorotyntsev, A. V., Vorotyntsev, I. V., 2019. Novel Composite Membranes Based on Chitosan Copolymers with Polyacrylonitrile and Polystyrene: Physicochemical Properties and Application for Pervaporation Dehydration of Tetrahydrofuran. *Membranes* 2019, Vol. 9, Page 38 9, 38. <https://doi.org/10.3390/MEMBRANES9030038>
- Petukhov, A.N., Atlaskin, A.A., Kryuchkov, S.S., Smorodin, K.A., Zarubin, D.M., Petukhova, A.N., Atlaskina, M.E., Nyuchev, A. V., Vorotyntsev, A. V., Trubyanov, M.M., Vorotyntsev, I. V., Vorotyntsev, V.M., 2021. A highly-efficient hybrid technique – Membrane-assisted gas absorption for ammonia recovery after the Haber-Bosch process. *Chemical Engineering Journal* 421, 127726. <https://doi.org/10.1016/J.CEJ.2020.127726>
- Petukhov, A.N., Atlaskin, A.A., Smorodin, K.A., Kryuchkov, S.S., Zarubin, D.M., Atlaskina, M.E., Petukhova, A.N., Stepakova, A.N., Golovacheva, A.A., Markov, A.N., Stepanova, E.A., Vorotyntsev, A. V., Vorotyntsev, I. V., 2022. An Efficient Technique for Ammonia Capture in the Haber–Bosch Process Loop—Membrane-Assisted Gas Absorption. *Polymers* 2022, Vol. 14, Page 2214 14, 2214. <https://doi.org/10.3390/POLYM14112214>
- Rahmani, M., Mokhtarani, B., Rahmanian, N., 2023. High pressure adsorption of hydrogen sulfide and regeneration ability of ultra-stable Y zeolite for natural gas sweetening. *Fuel* 343, 127937. <https://doi.org/10.1016/J.FUEL.2023.127937>
- Rayer, A. V., Sumon, K.Z., Sema, T., Henni, A., Idem, R.O., Tontiwachwuthikul, P., 2012. Part 5c: Solvent chemistry: Solubility of CO<sub>2</sub> in reactive solvents for post-combustion CO<sub>2</sub>. *Carbon* 50, 467–484. [https://doi.org/10.4155/CMT.12.47/SUPPL\\_FILE/SUPPL\\_DATA.DOCX](https://doi.org/10.4155/CMT.12.47/SUPPL_FILE/SUPPL_DATA.DOCX)
- Robeson, L.M., 2008. The upper bound revisited. *J Memb Sci* 320, 390–400. <https://doi.org/10.1016/J.MEMSCI.2008.04.030>

- Rochelle, G.T., 2024. Air pollution impacts of amine scrubbing for CO<sub>2</sub> capture. *Carbon Capture Science & Technology* 11, 100192. <https://doi.org/10.1016/J.CCST.2024.100192>
- Shirazi, M., Ghasemi, A., Šimurina, J., 2022. The impact of the North American shale gas technology on the US' energy security: the case of natural gas. *International Journal of Sustainable Energy* 41, 810–831. <https://doi.org/10.1080/14786451.2021.1979002>
- Si, X., Lu, R., Zhao, Z., Yang, X., Wang, F., Jiang, H., Luo, X., Wang, A., Feng, Z., Xu, J., Lu, F., 2022. Catalytic production of low-carbon footprint sustainable natural gas. *Nature Communications* 2022 13:1 13, 1–9. <https://doi.org/10.1038/s41467-021-27919-9>
- Sidhikku Kandath Valappil, R., Ghasem, N., Al-Marzouqi, M., 2021. Current and future trends in polymer membrane-based gas separation technology: A comprehensive review. *Journal of Industrial and Engineering Chemistry* 98, 103–129. <https://doi.org/10.1016/J.JIEC.2021.03.030>
- Singh, R., Prasad, B., Ahn, Y.H., 2024. Recent developments in gas separation membranes enhancing the performance of oxygen and nitrogen separation: A comprehensive review. *Gas Science and Engineering* 123, 205256. <https://doi.org/10.1016/J.JGSCE.2024.205256>
- Smetannikov, V.P., Orlov, A.N., Malinin, N.N., Semenova, O.P., 2010. Method of producing xenon concentrate from natural combustible gas, products of its treatment including man-caused off gases and device to this end (versions). Patent RU 2,466,086.
- Struk, M., Kushkevych, I., Vítězová, M., 2020. Biogas upgrading methods: recent advancements and emerging technologies. *Rev Environ Sci Biotechnol* 19, 651–671. <https://doi.org/10.1007/S11157-020-09539-9/METRICS>
- Tikadar, D., Gujarathi, A.M., Guria, C., 2021a. Safety, economics, environment and energy based criteria towards multi-objective optimization of natural gas sweetening process: An industrial case study. *J Nat Gas Sci Eng* 95, 104207. <https://doi.org/10.1016/J.JNGSE.2021.104207>
- Tikadar, D., Gujarathi, A.M., Guria, C., Al Toobi, S., 2021b. Retrofitting and simultaneous multi-criteria optimization with enhanced performance of an industrial gas-cleaning plant using economic, process safety, and environmental objectives. *J Clean Prod* 319, 128652. <https://doi.org/10.1016/J.JCLEPRO.2021.128652>
- Vorotyntsev, I. V., Drozdov, P.N., Shablikin, D.N., Gamajunova, T. V., 2006. Ammonia separation and purification by absorbing pervaporation. *Desalination* 200, 379–380. <https://doi.org/10.1016/J.DESAL.2006.03.382>
- Vorotyntsev, V.M., Drozdov, P.N., Vorotyntsev, I. V., 2009. High purification of substances by a gas separation method. *Desalination* 240, 301–305. <https://doi.org/10.1016/J.DESAL.2007.12.043>
- Vorotyntsev, V.M., Drozdov, P.N., Vorotyntsev, I. V., Smirnov, K.Y., 2006. Germane high purification by membrane gas separation. *Desalination* 200, 232–233. <https://doi.org/10.1016/J.DESAL.2006.03.307>
- Yahaya, G.O., Choi, S.-H., Ben Sultan, M.M., Hayek O Yahaya, A.G., Choi, S., B Sultan, M.M., Hayek, A., 2020. Development of Thin-Film Composite Membranes from Aromatic Cardo-Type Co-Polyimide for Mixed and Sour Gas Separations from Natural Gas. *Global Challenges* 4, 1900107. <https://doi.org/10.1002/GCH2.201900107>

- Yamada, H., Higashii, T., Chowdhury, F.A., Goto, K., Kazama, S., 2012. Experimental Study Into Carbon Dioxide Solubility And Species Distribution In Aqueous Alkanolamine Solutions. WIT Transactions on Ecology and the Environment 157, 515–523. <https://doi.org/10.2495/AIR120451>
- ZOU, C., XIONG, B., XUE, H., ZHENG, D., GE, Z., WANG, Y., JIANG, L., PAN, S., WU, S., 2021. The role of new energy in carbon neutral. Petroleum Exploration and Development 48, 480–491. [https://doi.org/10.1016/S1876-3804\(21\)60039-3](https://doi.org/10.1016/S1876-3804(21)60039-3)